

# Effects of sound on flow separation from blunt flat plates

R. Parker\* and M. C. Welsh†

The effect of sound on the flow around plates with semicircular or square leading edges and square trailing edges located in a low turbulence open jet has been studied. In all circumstances the length of the leading edge separation bubbles associated with square leading edge plates was found to oscillate. When sound was applied to the flow around these plates, the leading edge shear layers reattached closer to the leading edge and the oscillations in bubble length occurred at the applied sound frequency, generating patches of concentrated vorticity in the boundary layers. These vorticity patches moved downstream near the plate surface and then beyond the trailing edge to form vortex cores in a street with a Strouhal number equal to the applied sound value. Sometimes these vortex streets are unstable and break down into streets with Strouhal numbers approaching those observed without sound. These effects of sound were not observed in the flow around plates with semicircular leading edges. Without sound, square leading edge plates of intermediate length did not shed regular vortex streets.

**Key words:** *Vortices, aero acoustics, flow separation, bluff bodies*

It has been known for many years that the flow around a bluff body involves unsteady fluid velocities and pressures near the body. Strouhal<sup>1</sup> discovered that the flow around cylinders is associated with the generation of sound whose frequency varies linearly with the flow velocity.

A considerable effort has been devoted to studying the flow around circular cylinders, for example by Gerrard<sup>2-6</sup>, Bearman<sup>7,8</sup>, and others, and rectangular prisms<sup>9-11</sup> which relate to buildings and transport vehicles. Nakaguchi, Hashimoto and Muto<sup>12</sup> studied the vortex shedding characteristics and the shear layers which separate from the leading edges of bluff bodies with rectangular cross-sections in low turbulence flow. They found that the vortex shedding frequency increases suddenly as the chord to thickness ratio is increased through 2.8 when the shear layers, which separate from near the plate's leading edge, reattach onto the body. Bearman and Trueman<sup>13</sup> made a similar study of the flows around bluff bodies with rectangular cross-sections and chord to thickness ratios up to 1.2. They observed that the trend of reducing Strouhal number with increasing plate chord is consistent with Gerrard's hypothesis<sup>4,5</sup> which relates the rate at which circulation is fed from the shear layers to the vortex shedding frequency.

Sarpkaya<sup>14</sup> recently reviewed the published work on vortex induced vibration which included experimental studies and mathematical models of the mechanisms by which the vortex streets are

formed (see for example Sarpkaya and Shoaff<sup>15</sup>, Gerrard<sup>6</sup>, and Clements<sup>16</sup>).

Mechanical vibration of a body causes appreciable changes to the vortex shedding frequency<sup>17,18</sup> when the so-called 'lock-on' phenomenon occurs. Under these circumstances the vortex shedding frequency can change by as much as 25% of the value observed without vibration. Furthermore, the 'lock-on' is associated with a marked increase in the correlation of the vortex shedding in the wake.

An analogous vibration and 'lock-on' is achieved when, instead of the body vibrating, the fluid vibrates as an acoustic motion<sup>19-23</sup>. This phenomenon occurs when the vortex shedding frequency coincides with the acoustic resonant frequency of the space surrounding the body in a duct. In most examples of acoustic resonance the vortex shedding frequency remains almost constant and equal to the acoustic frequency as flow velocity is increased through the resonance, resulting in a fall in the vortex shedding Strouhal number. A further consequence of an acoustic resonance is that the vortex shedding process approaches two dimensional flow<sup>21</sup>.

Recently, Welsh and Gibson<sup>24</sup> discovered that a plate with square leading and trailing edges having a chord/thickness ratio of 5 could excite acoustic resonances in a duct with acoustic Strouhal numbers between 0.10 and 0.12 and also in another range between 0.18 and 0.21 with corresponding changes in the vortex shedding frequency. Nakaguchi, Hashimoto and Muto<sup>12</sup> showed that natural shedding from plates of similar proportions as that used by Welsh and Gibson<sup>24</sup> gave a Strouhal number of approximately 0.1 which clearly corresponds to the resonant conditions generated in a duct at the lower Strouhal numbers. The resonances generated at the higher Strouhal numbers (0.18 to 0.21) represent a

\* Department of Mechanical Engineering, University College of Swansea, Singleton Park, Swansea SA2 8PP, UK

† Division of Energy Technology, Commonwealth Scientific and Industrial Research Organization, Melbourne, Australia  
Received on 8 October 1982 and accepted for publication on 17 December 1982

change of nearly 100% in the vortex shedding frequency and imply a change in the flow regime. A 'feed-back' effect was examined and modelled by Archibald<sup>25</sup>, but his theory did not explain the fluid mechanics associated with the locking of the vortex shedding to the acoustic field.

Several workers<sup>3,4,26</sup> have examined the effect of applied sound on the flow around circular cylinders in non-resonant conditions at Reynolds numbers, based on cylinder diameter and upstream flow velocity, in the range 2000 to 50 000. It was always found that sound introduced close to the frequency of the shear layer transition waves, first reported by Bloor<sup>27</sup>, augmented the instabilities occurring naturally in the shear layers and only weakly affected the frequency at which vortices formed in the wake; sound applied at other frequencies had no effect on the shear layer instability waves or the vortex shedding frequency. Several workers<sup>6,15,16</sup> have shown that it is possible to predict accurately the vortex

shedding frequency from circular cylinders without accounting for any instability mechanisms in the shear layers. Nagano, Naito and Takata<sup>28</sup> achieved similar results for plates with rectangular cross-sections. Peterka and Richardson<sup>26</sup> also found that sound applied around a circular cylinder transverse to the flow direction caused increased discretization of vorticity within the separated shear layers. They suggested that this was one factor responsible for reducing the length of the vortex formation region.

Since vortex shedding and shear layer fluctuations are associated with many cases of flow induced mechanical and acoustic vibration, an experimental study of the flow around a series of flat plates has been undertaken to establish the fluid mechanics of the interaction between flow and resonant acoustic vibration. This paper presents the results of an investigation into the effect of sound on the separated flows from plates located in an open jet using a sound source (loud-speakers) which is

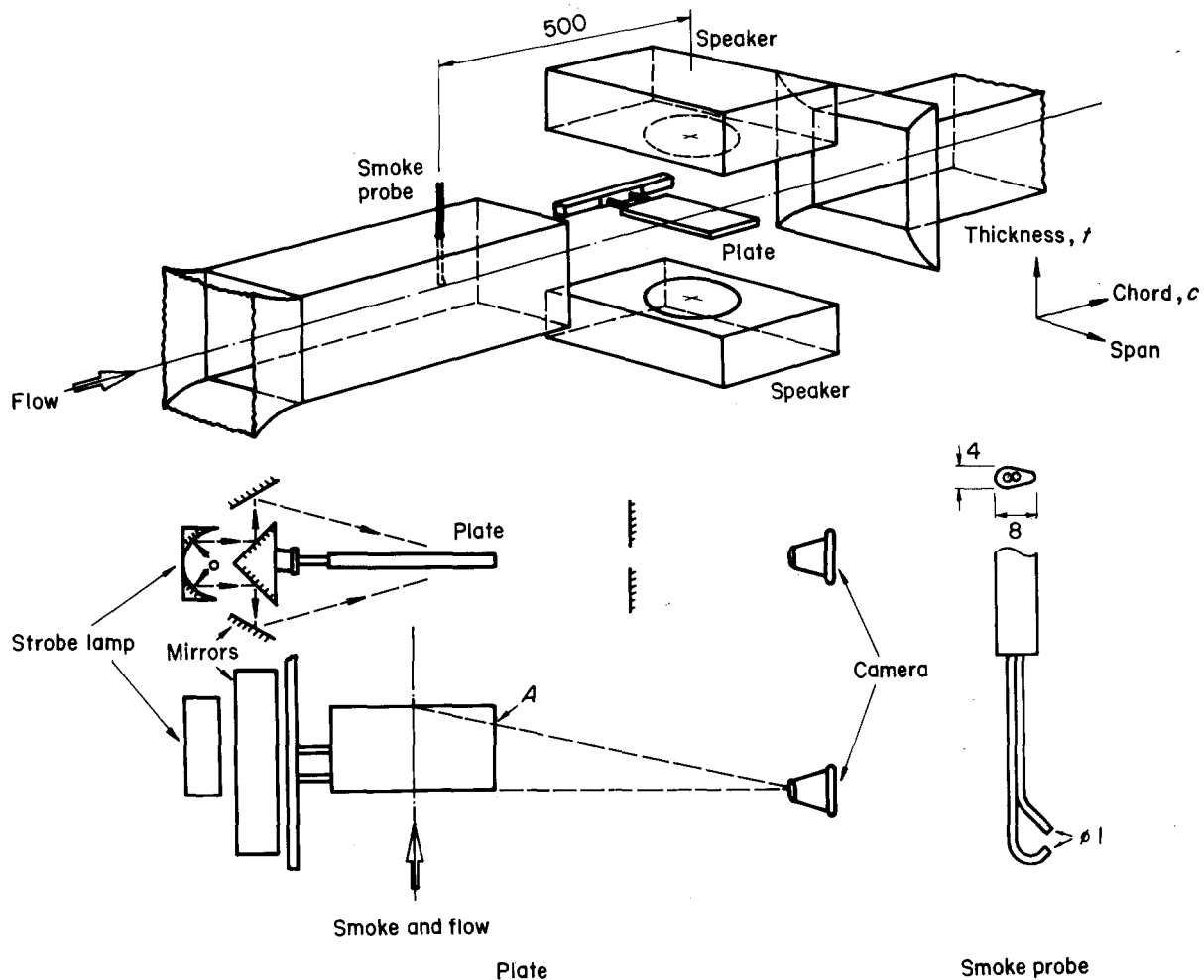
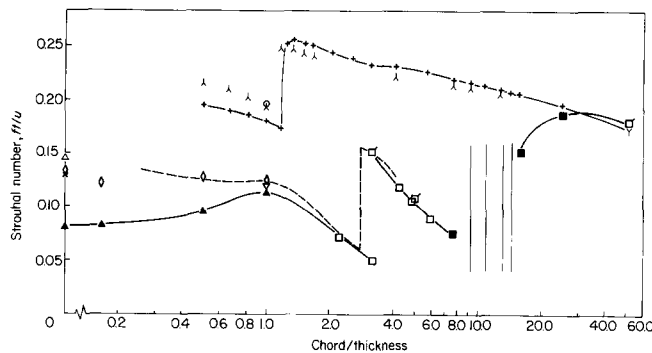


Fig 1 Test apparatus. 'A' apparent location of smoke at plate's trailing edge in mid-span plane

#### Notation

$f$  Vortex shedding frequency or acoustic resonant frequency  
 $t$  Plate thickness  
 $U$  Mean flow velocity upstream of plate

$St$  Strouhal number ( $ft/U$ )  
 $c$  Overall length of a plate in the flow direction including the semi-circular leading edges where appropriate



**Fig 2** Vortex shedding Strouhal number for flat plates at zero incidence without sound applied.  $Re = 14\,800$  to  $31\,100$

- ▲ square leading edge narrow spectral peak without end plates  $t = 12$
- ◇ square leading edge narrow spectral peak with end plates  $t = 12$
- square leading edge narrow spectral peak with and without end plates  $t = 12$
- ◻ square leading edge narrow spectral peak with and without end plates  $t \approx 6$
- square leading edge broad spectral peak with and without end plates  $t = 12$
- | square leading edge no spectral peak with and without end plates  $t = 12$
- + semi-circular leading edge without end plates  $t = 12$
- λ semi-circular leading edge with end plates  $t = 12$
- γ semi-circular leading edge with and without end plates  $t \approx 6$
- circular cylinder with end plates  $t = 12$

Nakaguchi *et al* ---; Roshko ×; Fage & Johansen, △; Vickery, ▽

virtually independent of changes induced in the flow by the sound. The maximum sound levels used were much lower than those encountered when vortex shedding excites acoustic resonances in closed ducts, but the use of an independent sound source facilitates control over frequency and amplitude of the sound in a manner which is not possible in a duct. The interaction between the sound and the flow represents the 'feed back' effect of sound on the acoustic source during resonance.

### Experimental apparatus and procedure

The test apparatus (Fig 1) was a small open jet wind tunnel with a working section  $244 \times 244$  mm at the outlet. The mean velocity in the jet was uniform within 0.5%, while the longitudinal turbulence intensity was 0.2%; the major spectral components lie between 0.1 Hz and 150 Hz.

All the test plates had square trailing edges and either semicircular or square leading edges. Each plate had a span equal to the jet width and was mounted at zero incidence across the centre of the jet. Without applied sound, plates were tested both with and without end plates; when fitted, these extended upstream a minimum distance of two test plate thicknesses and downstream a minimum

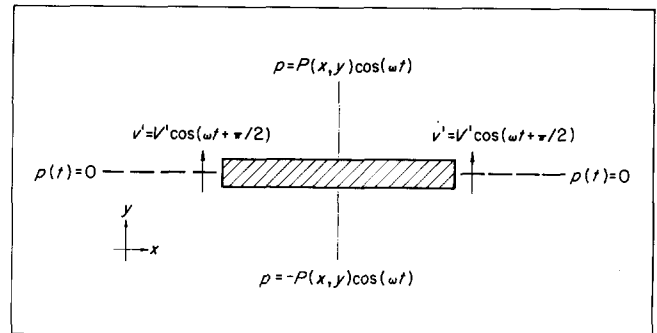


**Fig 3** Applied acoustic field in vicinity of plate; --- pressure nodes and velocity and displacement antinodes; — · — ·, velocity and displacement nodes in x-direction;  $p$  = acoustic pressure;  $P$  = maximum acoustic pressure;  $v'$  = acoustic velocity;  $V'$  = maximum acoustic velocity;  $\omega$  = acoustic frequency

distance of four test plate thicknesses<sup>29,30</sup>. The chord to thickness ratios ranged up to 52 (Fig 2) and most of the plates were nominally 12 mm thick; exceptions were the plates of longest chord, which were 5.75 mm thick, and two square leading edge plates 6.4 mm thick having the same chord to thickness ratios as two of the 12 mm thick plates (Fig 2).

Unsteady flows in the wakes of the plates were recorded with a hot wire sensor located downstream of the trailing edge and below the lower plate surface with the wire parallel to the plate span. Averaged spectra were obtained from the hot wire signals using a spectrum analyser and the recorded results are plotted with an uncalibrated linear amplitude scale.

Sound was applied by two 250 mm diameter loudspeakers connected in antiphase and placed symmetrically above and below the jet (Fig 1). A two channel power amplifier and a phase control circuit were used so that the relative levels and phases of each speaker could be adjusted to establish an acoustic pressure node (zero acoustic pressure) in the horizontal plane midway between the loudspeakers, ie in the plane of the plates. Sound frequencies typical of the resonant frequencies observed in closed ducts (150–900 Hz) were used; the characteristics of the acoustic field generated around the plate are shown in Fig 3. The distribution of the acoustic amplitudes near the plate in the mid-span plane is very similar to that for an acoustic  $\beta$ -mode in a duct<sup>31</sup>. The essential features are that all the acoustic pressures above the plate are in phase and  $180^\circ$  out of phase with the pressures below the plate. (The same is true of the acoustic velocities and displacements.) Peak pressure amplitudes occur at the mid-chord positions above and below the plate while zero pressure amplitudes, and therefore maximum acoustic velocities and displacements, occur on the centre plane upstream and downstream of the leading and trailing edges. The acoustic velocities and displacements are always zero at the mid-chord positions on the surface of the plate.

The sound field was monitored by two microphones. One was fixed below the jet and slightly upstream of the lower loudspeaker and was used as

a fixed reference for all tests. The other was fitted with a 2 mm diameter probe and mounted on a traversing arrangement located outside the jet. The open end of the probe was located in the mid-span plane. This microphone was used without flow to establish an acoustic pressure node in the plane of the plate, and to record and calibrate the amplitude of the acoustic pressures around the plate relative to the fixed microphone; it was removed for all tests with flow.

All the plates tested with sound were nominally 12 mm thick without end plates fitted. The effect of sound on the flows around longer plates ( $c/t > 16$ ) was not studied since the loudspeaker system (Fig 1) could not generate satisfactory sound fields surrounding these plates.

Flow visualization and the averaged spectra described above were used to determine the general flow properties. Smoke was generated by introducing ammonia and sulphur dioxide gases independently into the flow using techniques developed by Bassett and Fowler<sup>32</sup>. These gases react exothermally forming ammonium sulphite powder which clearly disclosed changes in the flow patterns around the plates when sound was applied at freestream velocities up to  $70 \text{ m s}^{-1}$ . Smoke probes (which were retracted out of the flow when not in use) were located 500 mm upstream of the plates and were

introduced from above and below the plates so that they did not intersect the stagnation streamline upstream of the plate. The smoke was illuminated with stroboscopic or single flashlight, reflected into the flow by a system of mirrors (Fig 1). This permitted detailed examination of the flow associated with the spectral spikes recorded in the averaged spectra and provided an independent check of the vortex shedding frequencies. The flow visualization and hot wire measurements for each plate were made at the same flow velocity.

Permanent records of the flow patterns were obtained by single flash photographs with the flash light fired at predetermined points in the acoustic cycle. During the investigation of *natural vortex shedding*, the flow was observed first with no sound and then with sound at a frequency corresponding to the mean vortex shedding frequency. The sound level was gradually increased until the visual image, observed using light strobed at the sound frequency, became stationary; this always occurred at a level well below that at which the sound caused any other detectable changes in the flow around the plates. Sometimes small amounts of water were introduced onto the plate surface (by a hand held tube) to provide an indication of the mean position of the boundary layer separation and reattachment.

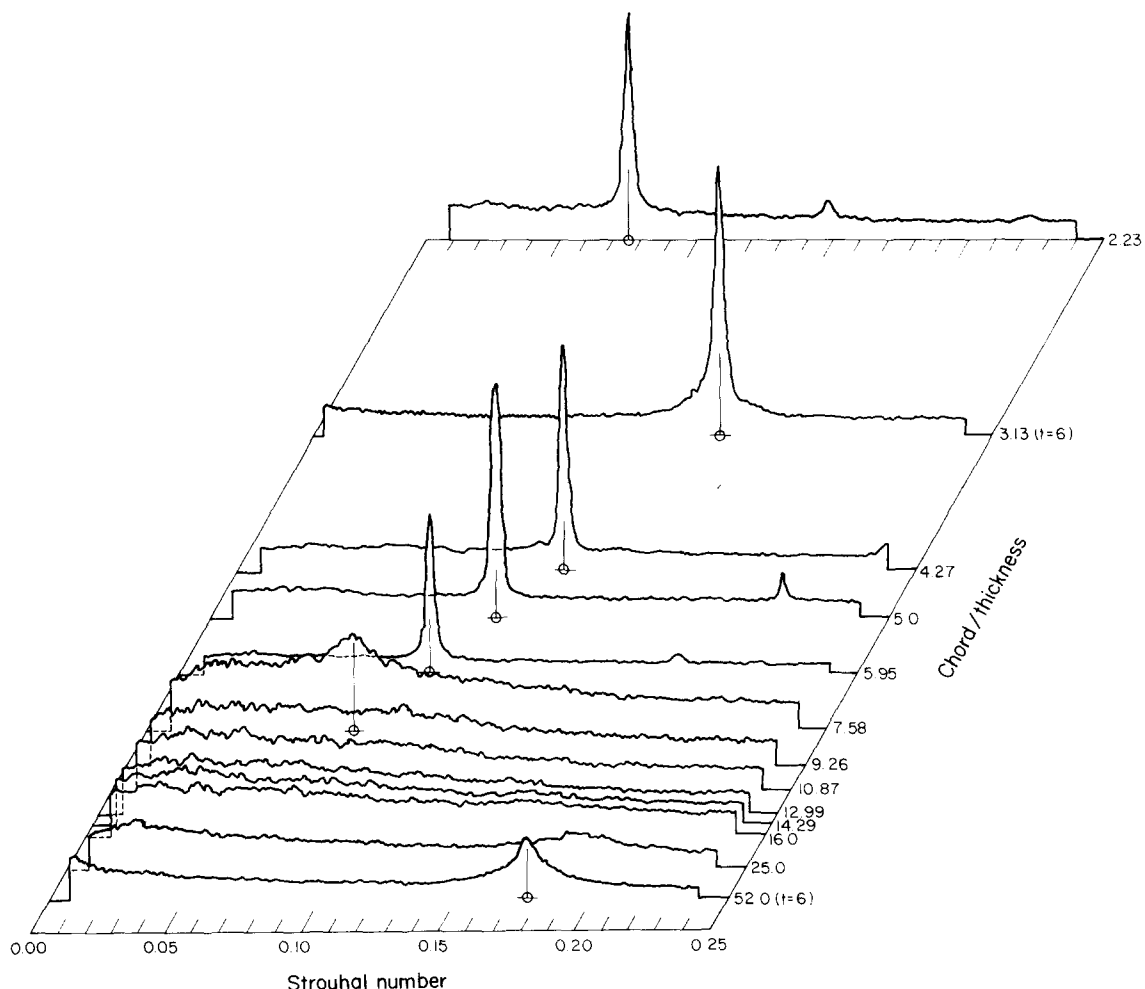


Fig 4 Spectra of hot wire located in wake from plates with square leading and trailing edges.  $Re = 14\,800$  to  $31\,100$

The results of flow visualization studies must be interpreted with caution particularly when an acoustic field is superimposed on the flow or when there is unsteadiness in the flow. The existence of fluctuations in any flow region can be indicated by stroboscopic illumination of smoke introduced into the flow but the precise configuration of the shear layers, vortices, etc cannot be deduced from photographs of the smoke patterns alone. Hama<sup>33</sup> has illustrated that streaklines originating from a sinusoidal oscillation in a shear flow indicate apparent vortices when he believed there were no vortices present, but Michalke<sup>34</sup> has since shown that there were concentrations of vorticity in the flow model used. However, in spite of these uncertainties, some information can be deduced with confidence, in particular if the smoke is viewed with stroboscopic light; the frequency at which a stationary pattern is seen is the frequency at which the fluctuations take place.

### Results without applied sound

The measured vortex shedding frequencies of all the plates without sound (natural vortex shedding) are given in Fig 2 as the relationship between the vortex shedding Strouhal number and the chord/thickness ratio. Some of the recorded spectra of the hot wire signals for plates with square leading edges are shown in Fig 4. These spectra are plotted to an uncalibrated linear amplitude scale. For approximately half of the plates tested, spectra were recorded at several flow velocities equivalent to a Reynolds number range of 14 800 to 31 100 based on plate thickness. Since these results showed that Reynolds number had no detectable effect in this range, the remaining tests were made at a Reynolds number of approximately 23 700, ie approximately  $29.5 \text{ m s}^{-1}$ .

The results (Fig 2) show clearly that plates with square leading edges shed wakes in four different regimes characterized by discontinuities in

the relationship between the Strouhal number and the chord/thickness ratio. All the plates with  $c/t$  less than 7.6 shed vortices at discrete frequencies. The vortex shedding Strouhal numbers of plates with chord to thickness ratios less than 3 are increased by the addition of end plates. The shortest plate used in the present test ( $c/t = 0.055$ ) is compared with results obtained by Fage and Johansen<sup>35</sup> and Roshko<sup>36</sup> for thin plates normal to the flow. These data appear at the extreme left of Fig 2. It should be noted that the present results have not been subjected to any form of correction for blockage effects.

Observing the flow over the plate with  $c/t = 2.23$  confirmed results by Nakaguchi *et al*<sup>12</sup> that the leading edge shear layers on each side of the plate interact directly to form the alternating vortices downstream of the plate's trailing edge. The longest plate shedding vortices in this first regime (regime 'a') was a 12 mm thick plate with  $c/t = 3.16$ , while a 6.4 mm thick plate with the same  $c/t$  ratio clearly belongs to the second regime (regime 'b'). When end plates were fitted to the 12 mm thick plate, vortices were shed intermittently in both regimes.

The second vortex shedding regime applies to values of  $c/t$  from 3.2 to 7.6 of which the two plates with  $c/t = 5$  are typical; here the 6.4 and 12 mm thick plates gave the same Strouhal numbers and the presence of end plates had a negligible effect. All the plates shedding vortices in this regime emitted clearly audible sound at the vortex shedding frequency (also observed by Gerrard<sup>2</sup>). The flow around the 12 mm thick plate with  $c/t = 5$  is illustrated throughout one vortex shedding cycle in Fig 5. The illustrations were traced from a series of photographs, similar to those illustrated in Fig 6(c), spaced at  $36^\circ$  intervals throughout the cycle. A smoke stream was introduced into the flow either above or below the centre line of the plate so that the dense white smoke traced predominantly irrotational fluid while the grey smoke traced fluid from within the

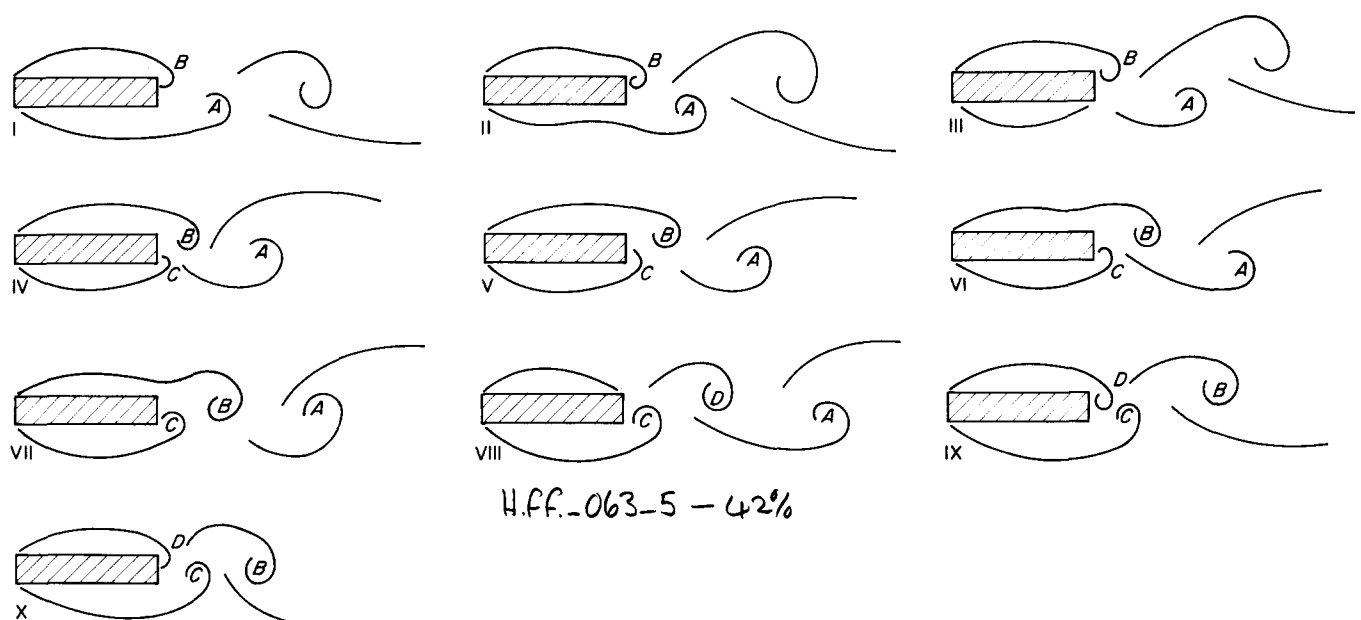
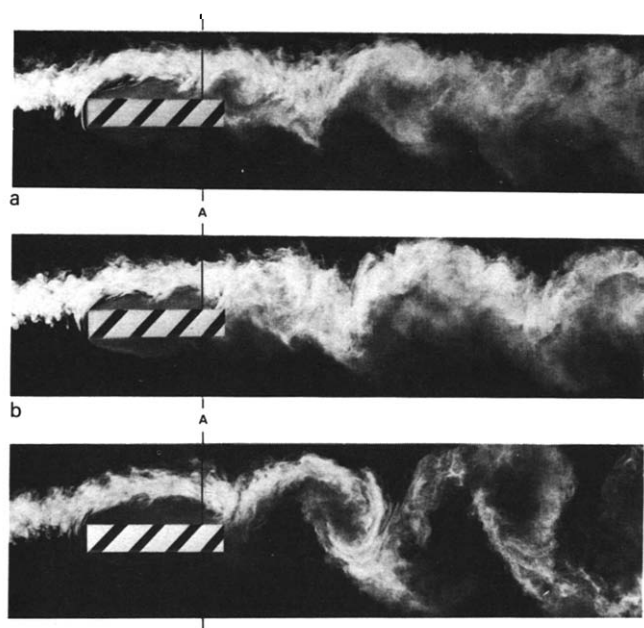


Fig 5 Vortex shedding cycle at  $36^\circ$  increments for square leading edged plate with  $c/t = 5$ ,  $Re = 26\,500$



**Fig 6** Flow around a square leading edged plate with and without sound applied. (a) sound level at mid-chord = 42 Pa(rms) and applied sound Strouhal number = 0.206. (b) sound level at mid-chord = 43 Pa(rms) and applied sound Strouhal number = 0.204, 180° out of phase with (a). (c) without applied sound, vortex shedding Strouhal number = 0.106. 'A', location of trailing edge at mid-span (Fig 1);  $c/t = 5$ ,  $Re = 26\,600$

separation bubble (Fig 6). The introduction of smoke into the flow did not change the frequency of the sound generated by the vortex street; if, however, the smoke probe crossed the stagnation streamline then the sound frequency increased by 1%.

Since the smoke was located in the mid-span plane and the camera was aligned with the plate's leading edge, a small region downstream of the plate's trailing edge was obscured in the photographs (Fig 1). The lines on Fig 5 in the obscured region were drawn after observing the flow with stroboscopic light and the lines on Figs 6 and 7 indicate the position of the trailing edge in the mid-span plane.

The series of tracings in Fig 5 show that the reattachment of the leading edge shear layers (first observed by Nakaguchi *et al*<sup>12</sup>), during the shedding of a vortex is intermittent. This process is common to all the plates in regime 'b' and is not significantly influenced by the presence of end plates.

The process of vortex street generation is important when relating the interaction between sound and vorticity<sup>37</sup> and is therefore described below for plates in regime 'b'. The first tracing (Fig 5) shows vortex A moving downstream after forming from the lower surface shear layer while vortex B, formed from the upper surface shear layer, is already well developed. The second and third tracings show fluid from the upper shear layer and irrotational fluid from further away being drawn into the region between A and B. The fluid from the shear layer causes vortex B to grow slowly and increase in total circulation, while A continues to move downstream.

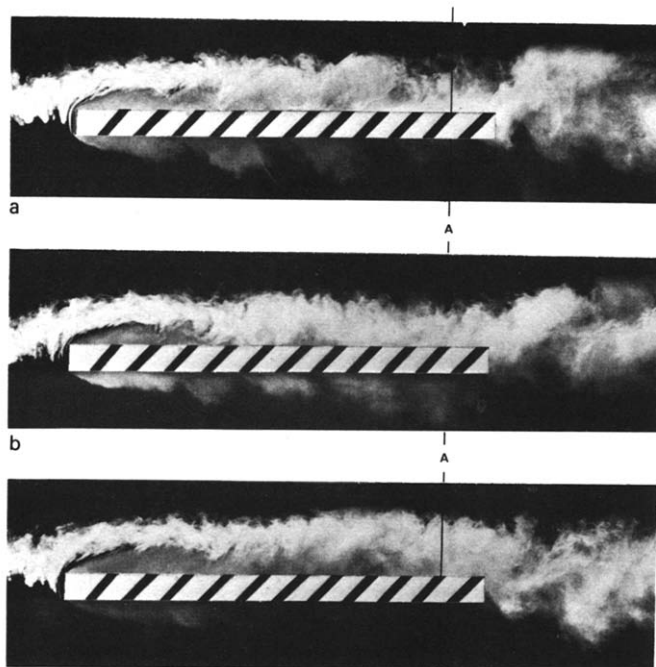


**Fig 7** Flow around a square leading edged plate with and without sound applied. (a) sound level at mid-chord = 29 Pa(rms) and sound Strouhal number = 0.176. (b) sound level at mid-chord = 44 Pa(rms) and sound Strouhal number = 0.244. (c) without applied sound; 'A', location of trailing edge at mid-span (Fig 1);  $c/t = 16$ ,  $Re = 24\,000$

During this period the lower shear layer deflects away from the centre line downstream of B and towards the centre line upstream. As B is very close to the trailing edge the result is that the lower shear layer is drawn in until it touches the underside of the plate at the trailing edge (tracing number III). This causes some fluid to move upstream into the separation bubble<sup>‡</sup> while some moves across between the trailing edge and vortex B.

The resultant growth of the lower separation bubble causes the reattachment position to move downstream allowing fluid with high vorticity to begin forming a new vortex C near the lower corner (tracing number IV) and vortex B starts to be displaced from its formation position. The fifth, sixth and seventh tracings show B moving away downstream while vortex C becomes stronger, and the second half of the cycle proceeds with reattachment on the upper surface (tracing number VIII) followed by detachment of vortex C and formation of vortex D (tracing numbers IX and X). This sequence was observed for all square leading edge plates between  $c/t = 3.2$  and 7.6.

Several photographs (eg Fig 6(c)) show that small diverging waves appear to exist in the smoke patterns just downstream of the leading edge. These regions are areas in which shear layer instabilities might be expected, leading to a breakdown into turbulence. The smoke patterns suggest that turbulence

<sup>‡</sup> Bradshaw and Wong<sup>38</sup> observed a similar division of the reattaching shear layer

occurs shortly after these waves cease to be definable.

The spectral peak for  $c/t = 7.6$  (Fig 4) was noticeably wider and less clearly defined than for plates with lower  $c/t$ . However, the corresponding Strouhal number falls on the same curve in Fig 2 applying to shorter plates and this plate proved to be the threshold of the change to the third vortex shedding regime 'c'. When the plate with  $c/t = 9.26$  was installed, spectra were recorded for sensor positions ranging from one plate thickness to 20 plate thicknesses downstream of the trailing edge. The spectra associated with all these sensor positions had no dominant spectral peaks. The sensor position was therefore standardized for all the longer plates at the position used for the  $c/t = 7.6$  plate (7 plate thicknesses downstream of the trailing edge). The spectra (Fig 4) show a very broad peak at  $c/t = 25$  and a more distinct one at  $c/t = 52$ . Further examination of the plates with  $c/t = 16$  and 25 showed that identifiable broad peaks could be found when the sensor was moved closer to the plate (2.9 plate thicknesses downstream of the trailing edge); the Strouhal numbers shown in Fig 2 were obtained from these spectral peaks. The reappearance of a peak indicates a gradual change to a fourth regime 'd' as  $c/t$  increases from about 16. Here the vortex shedding becomes more regular and the Strouhal number approximates the values obtained for plates of similar proportions with semicircular leading edges; the results are identical, within experimental accuracy, at  $c/t = 52$ . The addition of end plates to all the plates in regimes 'c' and 'd' ( $c/t > 7.6$ ) had a negligible influence on the associated vortex shedding frequencies shown in Fig 2.

Flow visualization studies showed that for all plates with  $c/t$  greater than 7.6 and a square leading edge (eg Fig 7(c)) the separated shear layers always reattached to the plate. A series of flash photographs showed that the position of reattachment varied in a random manner with reductions in the separation bubble length always resulting in a quantity of fluid separating from the bubble and convecting downstream in the boundary layer. This process, although somewhat random in frequency, is similar to the regular process observed when sound is applied (Fig 8). There was no apparent connection between the fluctuations on the upper and lower surfaces. The 'patches' of fluid which separate from the bubble as it shortens contain concentrations of vorticity which tend to diffuse as they move along the plate towards the trailing edge.

The results for plates with semicircular leading edges show that only two regimes can be identified, separated by a jump in Strouhal number when  $c/t$  is approximately 1.2. Flow visualization showed that at  $c/t = 1.16$ , the flow separated from the curved surface and did not reattach, the two shear layers interacting directly to form the vortices behind the plate in the same way as for the shorter, square leading edge plates. Visualization of the flow over the plate with  $c/t = 1.33$  showed the vortices forming very close to the trailing edge. Due to the small physical sizes of the plates used in this study, the resolution achieved using the flow visualization techniques described above was not sufficient to

distinguish if the shear layer was reattaching at any time during the cycle.

The influence of end plates on the vortex shedding frequency for plates with semicircular leading edges is similar to that recorded for plates with square leading edges. For short plates ( $c/t \leq 1$ ), where the shear layers which separate from near the plate's leading edge do not reattach, the Strouhal number increases when end plates are fitted (Fig 2). With longer plates the reverse occurs and for very long plates ( $c/t > 10$ ) the end plates have a negligible effect.

All plates with semicircular leading edges and  $c/t$  greater than 1.25 emitted audible sound at the vortex shedding frequency, ie in the range 435 to 650 Hz at a flow velocity of 29.5 m/s. The plates close to the Strouhal number jump also emitted sound at a much higher frequency (2000–3000 Hz).

The frequency of vortex shedding from a 12 mm circular cylinder with end plates fitted was measured to provide a comparison with other published data. The resulting Strouhal number of 0.196 is consistent with data quoted by Blevins<sup>39</sup> and

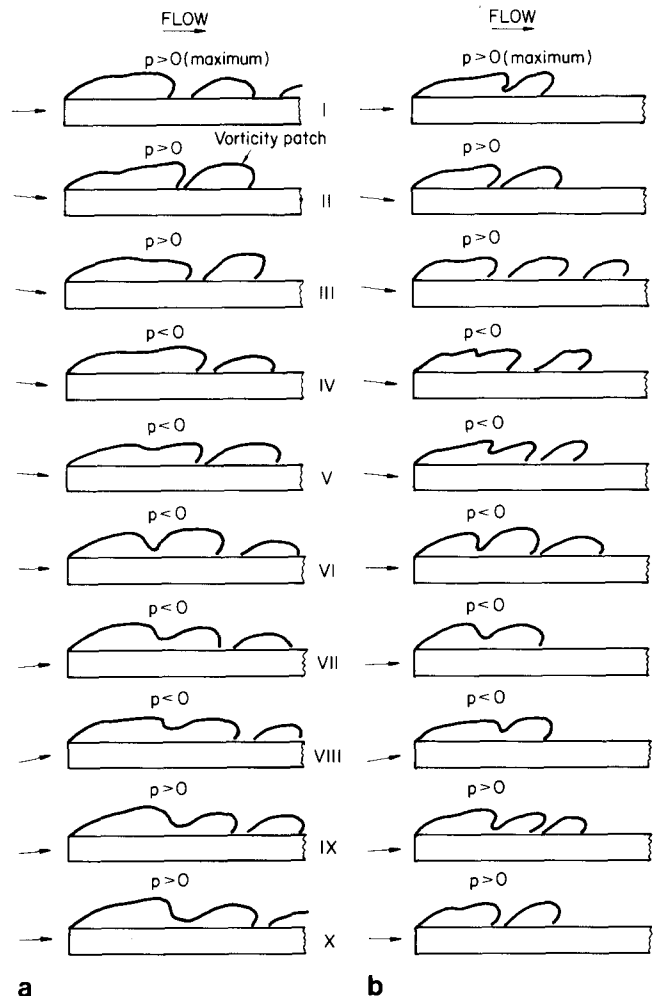


**Fig 8** Leading edge separation bubble oscillations at the acoustic frequency; tracings equi-spaced throughout cycle. (a), sound level at mid-chord = 29 Pa(rms) and sound Strouhal number = 0.176. (b) sound level at mid-chord = 46 Pa(rms) and sound Strouhal number = 0.244;  $c/t = 16$ ;  $Re = 24\,000$ ;  $p$  = acoustic pressure in the flow above the plate

Gerrard<sup>3</sup> for a Reynolds number of 23 700 and closely approximates the vortex shedding Strouhal number recorded for plates of the same chord with semicircular leading edges and square trailing edges.

### Results with sound applied

When sound is applied to the flow around a plate, the question if this significantly alters the interpretation of the smoke pictures must be examined. The range of acoustic pressures applied was up to 46 Pa(rms) and the associated velocity fluctuations and corresponding particle displacements never exceed 0.3 mm. Consequently, the sinusoidal displacements due to the sound field do not have a major effect on the shapes of the streamlines and the flow patterns can be compared directly with those observed without sound.

In general, the lengths of the leading edge separation bubbles in the flow direction were reduced when sound was applied to the flow surrounding plates with square leading edges. The reduction in the mean length of the leading edge separation bubbles was observed both by using smoke and by an independent observation using water droplets distributed on the surface of the plate. When sound was applied the water droplets migrated towards the leading edge indicating reduced pressure in the leading edge separation bubble with increased curvature in the shear layer and reattachment closer to the leading edge. The smoke also showed that the bubbles oscillated in length in a periodic manner at the sound frequency. Although the oscillation of the bubbles was regular and periodic with sound applied, the mechanism of the growth/division process was similar to the irregular growth/division process observed with no sound. The length of the separation bubbles in the flow direction reduced with increasing frequency, increasing sound pressure level and reducing flow velocity.

When sound is applied and reattachment occurs upstream of the trailing edge, discrete patches of high vorticity fluid (Fig 8) form in the plate boundary layers with one patch being generated on each side of the plate per acoustic cycle<sup>40</sup>. The vortex shedding Strouhal numbers, for plates with square leading edges with applied sound, are shown in Fig 9 for sound pressure levels ranging from 20 Pa(rms)<sup>\*</sup> for the plates of shorter chord up to 46 Pa(rms) for the plates of longer chord ( $c/t = 16$ ). The stability of the vortex street was assessed in the region up to 5 plate thicknesses downstream of the trailing edge of the plate. These results were obtained using flow visualization techniques which were not successful for applied sound Strouhal numbers greater than 0.25 due to the small scale of the structures generated at the sound frequency in the plate boundary layers. The influence of a regular distribution of vorticity patches in the plate boundary layers on the vortex shedding frequency depends on plate chord/thickness ratio and is detailed below.

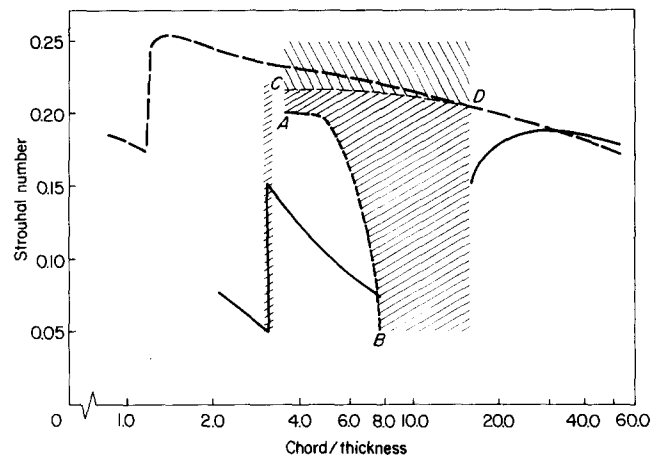
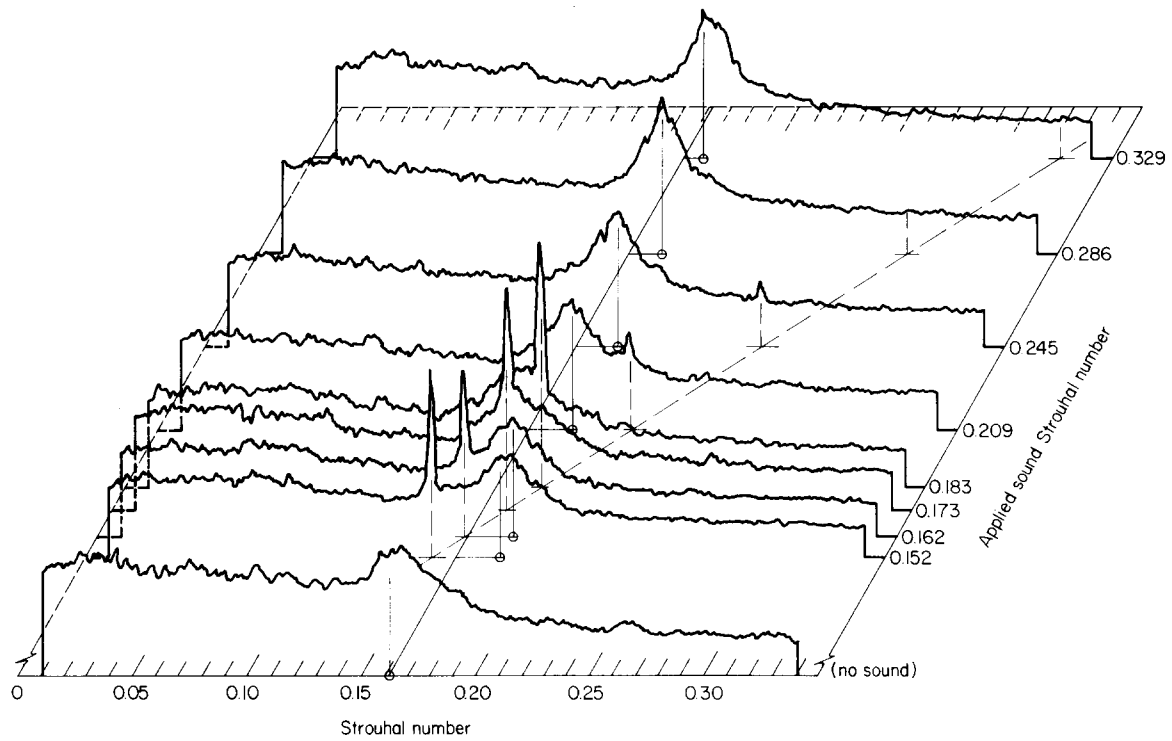


Fig 9 Vortex shedding and acoustic Strouhal numbers for flat plates at zero incidence with and without sound applied; sound level at mid-chord = 16 Pa(rms) for  $c/t < 3$  up to 46 Pa(rms) for  $c/t = 16$ ; —, square leading edges, no applied sound,  $Re = 14\,800$  to  $31\,100$ ; ---, semi-circular leading edges, no applied sound,  $Re = 23\,800$ ; ▨, square leading edges, stable vortex streets shed near the plate at applied sound Strouhal number,  $Re = 23\,800$  to  $26\,500$ ; ▩, square leading edges, unstable vortex streets shed near the plate initially at the applied sound Strouhal number,  $Re = 23\,800$  to  $26\,500$

Flow past the longest square leading edged plate in regime 'c' ( $c/t = 16$ ) is shown in Figs 7(a) and 7(b) with sound applied at acoustic Strouhal numbers of 0.176 and 0.244 respectively. The vorticity patches within the boundary layers are distributed along the upper and lower surfaces of the plates. The patterns on the lower surface are  $180^\circ$  out of phase with those on the upper surface because they are associated with the acoustic field on each side of the plate. Tracings in Fig 8 were obtained by similar methods to those described previously. An indication of the oscillating angle of attack of the approaching flow induced by the acoustic field is also shown and the first tracing in each sequence is within  $18^\circ$  of the maximum acoustic pressure above the plate. The positions where the shear layers reattach to the plate surface are seen to be much closer to the leading edge when sound is applied (see Fig 7(c) for no sound). The minimum bubble length occurs at approximately maximum acoustic pressure above the plate for both frequencies. The oscillation in bubble size consists of the bubble length increasing steadily until the bounding shear layer part way along the bubble deflects towards the plate surface and reattaches (tracing numbers I and X in Fig 8). This splits the bubble into two sections with the upstream section beginning to grow again, entraining fluid with high vorticity from the shear layer, and the downstream section moving as a discrete 'patch' of fluid with concentrated vorticity in the boundary layer. Visual studies of the flow using stroboscopic light show that although the vorticity patches diffuse as they move with the plate boundary layer flows, when sound is applied they reach the trailing edge alternately on each side of the plate.

<sup>\*</sup> All sound levels are for the mid-chord position





**Fig 10** Spectra of hot wire located in wake from a square leading edged plate with sound applied at 20 Pa(rms) at mid-chord; hot wire located 2.9 plate thicknesses downstream of trail edge;  $c/t = 16$ ;  $Re = 23\,900$ ; — natural shedding; — · — applied sound stimulus

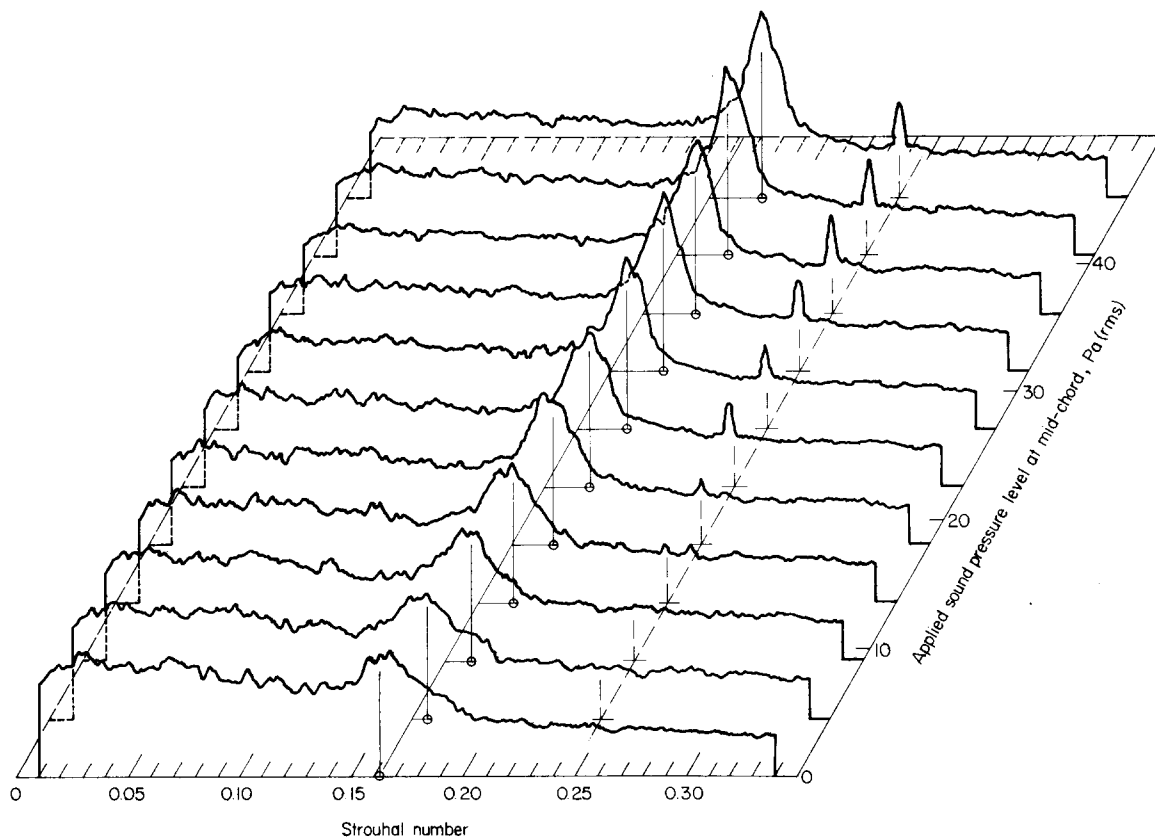


**Fig 11** Spectra of hot wire located in wake from a square leading edged plate with sound applied at a Strouhal number of 0.247 and varying pressure level; hot wire located 2.9 plate thicknesses downstream of trailing edge;  $c/t = 16$ ;  $Re = 23\,900$ ; — natural shedding; — · — applied sound stimulus

For all plates in regime 'c', sound applied at acoustic Strouhal numbers ranging from 0.05 to 0.25 generated one vorticity patch, similar to those shown in Figs 7(c) and 7(b), in each boundary layer per acoustic cycle. These patches were shed alternately from the trailing edge on each side of the plate at the sound frequency and eventually became vortex cores in the vortex street with a shedding Strouhal number equal to the acoustic Strouhal number (Fig 9). With applied sound Strouhal numbers falling below line CD on Fig 9, the resulting vortex street was stable near the plate (up to 5 plate thicknesses downstream of the trailing edge) but, at higher acoustic Strouhal numbers, the vortex street broke down and was replaced with a stable street of increased vortex spacing and a correspondingly lower Strouhal number. The region in the flow where the vortex street breaks down moves closer to the trailing edge with increasing applied sound Strouhal number. Averaged spectra obtained from a hot wire located at a fixed position (2.9 plate thicknesses downstream of the trailing edge) in the wake, with sound applied at Strouhal numbers ranging from 0.152 to 0.329, are shown in Fig 10. For applied sound Strouhal numbers between 0.152 and 0.2, the vortex street at the hot wire exists predominantly at the sound Strouhal number; this is consistent with the results of the flow visualization studies shown in Fig 9. As the sound Strouhal number approaches 0.2 some intermittent transition into a vortex street of lower Strouhal number, but slightly exceeding that observed without sound, occurs upstream of the hot wire. When the applied sound Strouhal number is increased beyond 0.2, the transition process is not intermittent and the vortex street continuously breaks down into a new street with larger spacing and lower frequency. The broad spectral peaks corresponding to the vortex streets following 'break down' have slightly higher Strouhal numbers than when no sound is applied and tend to narrow as the sound frequency increases up to the limit of the tests (Strouhal number = 0.329). Fig 11 shows averaged spectra, recorded by the hot wire located in the wake when the sound pressure level is progressively increased at a constant Strouhal number of 0.247. These data show the vortex street at the hot wire existing mostly, but not entirely, at Strouhal numbers slightly higher than those observed without sound and lower than the acoustic Strouhal number. This result is also consistent with the results of the flow visualization studies shown in Fig 9.

Flow past a square leading edge plate of intermediate length ( $c/t = 5$ ) in regime 'b' with sound applied at a Strouhal number of 0.206 is shown in Figs 6(a) and 6(b) and by the diagrams in Fig 12. An indication of the oscillating angle of attack of the approaching flow induced by the sound field is also shown. With no applied sound this plate shed vortices at a Strouhal number of 0.106 (Fig 6(c)), the shear layers only reattaching to the surface close to the trailing edge for a short period during each vortex shedding cycle (Fig 5). Consequently there were no discrete vorticity patches terminating on the plate surfaces at any time. The effect of the sound is to shorten the bubble so that the shear layers reattach

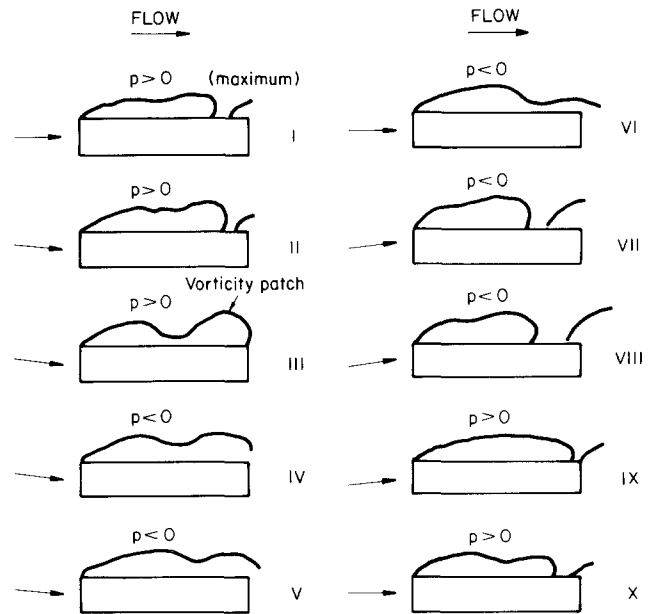


*Fig 12 Leading edge separation bubble oscillations at the acoustic frequency; tracings equi-spaced throughout cycle; sound level at mid-chord = 42 Pa(rms); applied sound Strouhal number = 0.206;  $c/t = 5$ ;  $Re = 26\,600$ ;  $p$  = acoustic pressure in the flow above the plate*

continuously (Figs 6(a) and 6(b)) but, in contrast to the longer plates, there is only one discrete vorticity patch (shed from the separation bubble) on each side of the plate at any one time (Fig 12). The leading edge separation bubbles almost reach the trailing edge before the shear layers are deflected towards the plate surface and reattach just downstream of the mid-chord position (tracing number VII in Fig 12). Minimum separation bubble length occurs when the acoustic pressures are negative above the plate, ie during the opposite half of the acoustic cycle than with that observed for longer plates.

Fig 13 illustrates averaged spectra obtained from a hot wire sensor located 2.9 plate thicknesses downstream of the trailing edge of a plate with  $c/t = 5$  for sound applied at Strouhal numbers ranging from 0.185 to 0.323. At a sound Strouhal number of 0.206 there are two spectral peaks, one at the sound frequency and the other at the natural shedding frequency. Fig 14 shows the effect of increasing the sound pressure level at a constant Strouhal number of 0.203. For levels greater than 25 Pa(rms) at the mid-chord position of the plate, there is only one spectral peak corresponding to a vortex street shedding at the sound frequency.

Observations of the flow, using stroboscopic light and the photographs similar to those shown in Figs 6(a) and 6(b), confirm that with the sound applied at a Strouhal number of 0.206 and a pressure level of 42 Pa(rms) the vorticity patches generated once per acoustic cycle became vortex cores in the vicinity of the trailing edge (up to 5 plate thicknesses downstream of the trailing edge). The vortex shedding Strouhal number is equal to the acoustic Strouhal number and is significantly greater than

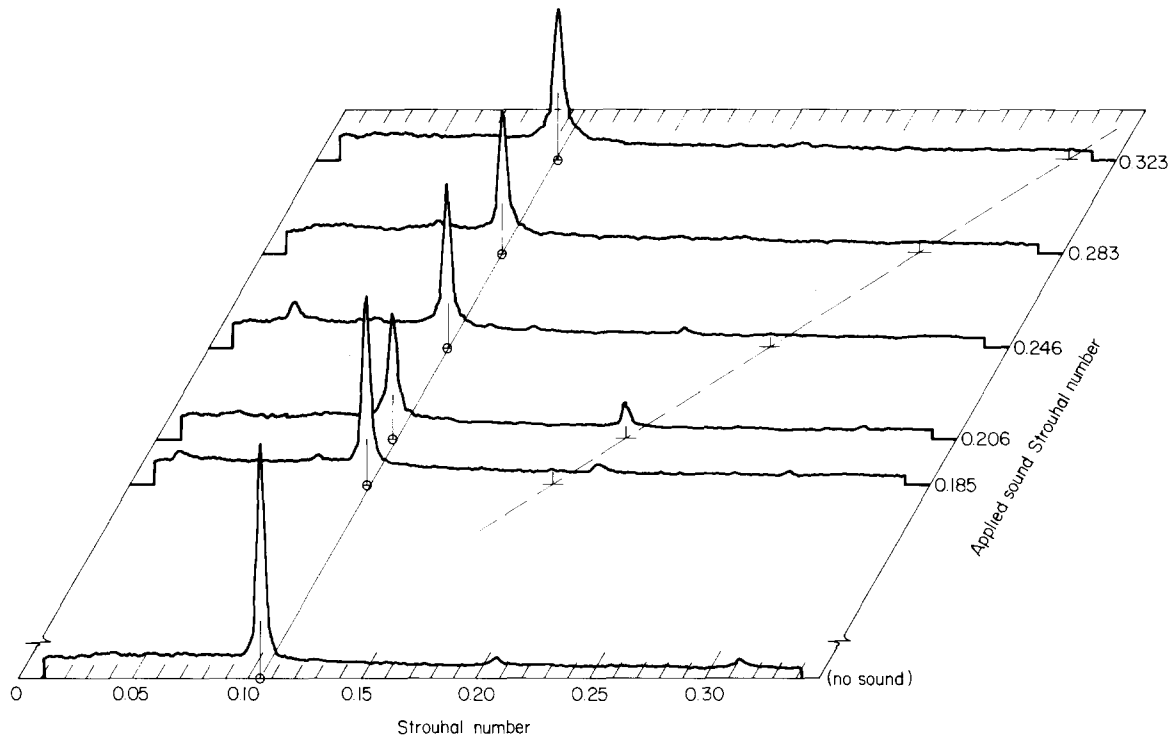


**Fig 13** Spectra of hot wire located in wake from a square leading edged plate with sound applied at 16 Pa(rms) at mid-chord; hot wire located 2.9 plate thicknesses downstream of trailing edge;  $c/t=5$ ;  $Re=24\,200$ ; — natural shedding; — · — applied sound stimulus

that observed without sound (compare Figs 6(a), 6(b) and 6(c) and Fig 9).

Sound applied over a range of frequencies to the flow around plates in this group (regime 'b') indicated there was a lower limit (line AB on Fig 9)

to the applied sound Strouhal number below which discrete vorticity patches were not generated, the limit being independent of the applied sound level. The shear layers on each side of the plate had not reattached to the plate's surfaces before the separ-

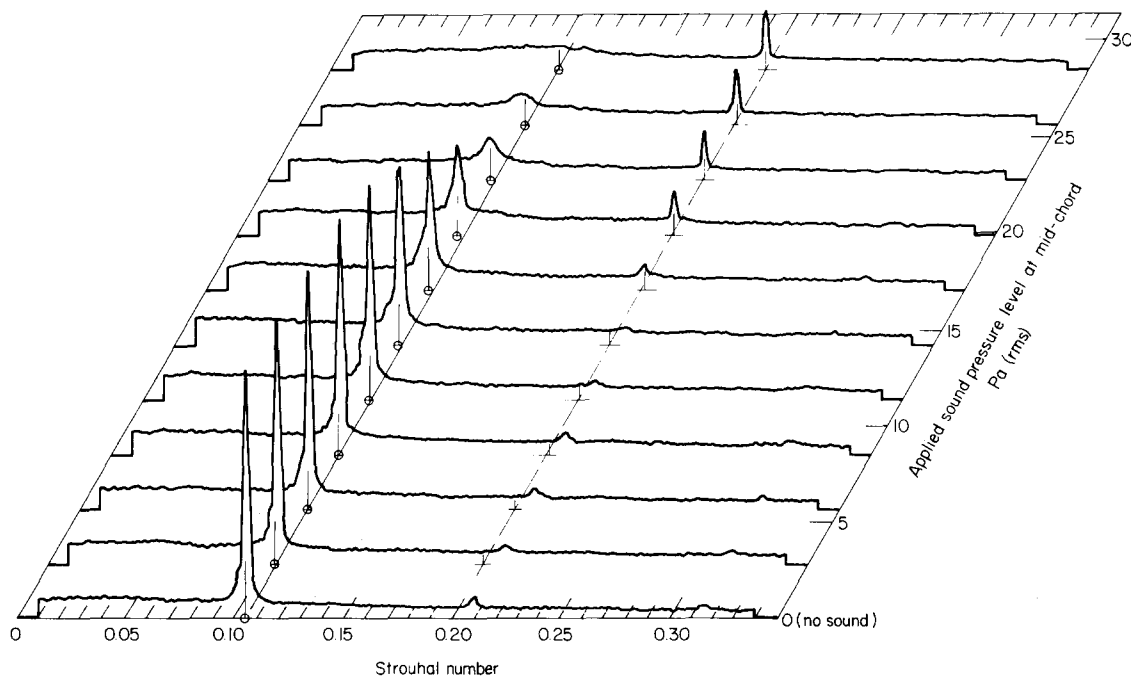


**Fig 14** Spectra of hot wire located in wake from a square leading edged plate with sound applied at a Strouhal number of 0.203 and varying pressure level; hot wire located 2.9 plate thicknesses downstream of trailing edge;  $c/t=5$ ;  $Re=26\,900$ ; — natural shedding; — · — applied sound stimulus

ation bubble grew beyond the trailing edge.\* At sound frequencies less than those corresponding to this limiting Strouhal number, visualization showed that the two leading edge separation bubbles interacted in the same way as when no sound was applied and vortices were shed at Strouhal numbers close to those observed without sound.

With sound applied at Strouhal numbers above line CD on Fig 9, visualization of the flow around plates in regime 'b' indicated vorticity patches being generated and initially shed at the sound Strouhal number. However, the Strouhal number of the vortex street within 3 plate thickness of the trailing edge was approximately equal to that observed without sound. This result is confirmed by the averaged spectra shown in Fig 13 and is a similar result to that observed for longer plates, described above, where the vortex street initially shed from the plate at the sound frequency breaks down into a street with increased vortex spacing.

The data shown in Fig 9 apply to vortex streets between the plate's trailing edge and 5 plate thicknesses downstream. Further downstream the vortex street can intermittently break down into a street of lower Strouhal number when sound is applied at frequencies corresponding to acoustic Strouhal numbers below line CD on Fig 9. Evidence of a

vortex street, with sound applied at a Strouhal number of 0.204, breaking down into a street of lower Strouhal number approximately 6 plate thicknesses downstream of the trailing edge is shown in Fig 6(b).

The shear layers, which separated from the square leading edges on short chord plates (regime 'a' with  $c/t < 3$ ) together with their associated vortex streets, did not change significantly when subjected to applied sound at acoustic Strouhal numbers ranging between 0.05 and 0.25 and sound pressure levels up to 16 Pa(rms) (Fig 9).

The longest plate which naturally sheds vortices in regime 'a' was the plate with  $c/t = 3.16$  with  $t = 12$  mm. This plate was found to respond to applied sound in a manner similar to plates of higher  $c/t$  ratios (natural shedding regime 'c'), shedding a stable vortex street at the sound frequency for all acoustic Strouhal numbers from 0.05 up to 0.22 (Fig 9).

For all the plates tested with semicircular leading edges ( $0.5 \leq c/t \leq 16$ ), the application of sound had no significant effect on the vortex shedding frequency. Averaged spectra from a hot wire sensor located 2.9 plate thicknesses downstream of the trailing edge of a plate with  $c/t = 16$  are shown in Fig 15. Sound applied with Strouhal numbers varying between 0.143 and 0.287 produced small spectral peaks at the sound frequency and negligible changes in the amplitude and frequency of the spectral peak corresponding to the main vortex shedding.

\* The maximum length of the bubble increases with reducing sound frequency.

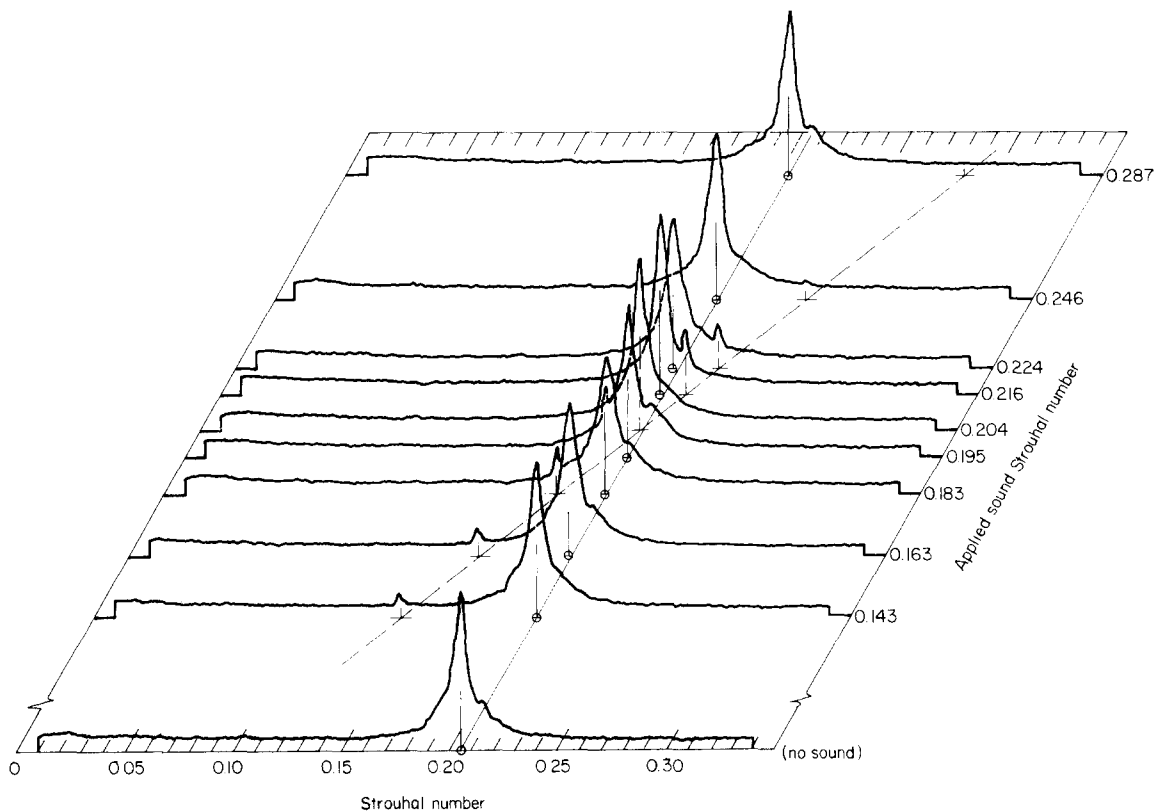


**Fig 15** Spectra of hot wire located in wake from a semi-circular leading edged plate with applied sound level at mid-chord = 20 Pa(rms); hot wire located 2.9 plate thicknesses downstream of trailing edge;  $c/t = 16$ ;  $Re = 24\,000$ ; — natural vortex shedding; — · — applied sound stimulus

## Discussion and conclusions

### Natural vortex shedding frequencies

The measured values of vortex shedding frequency have defined the relationships between the Strouhal number and plate dimensions for flat plates with square or semicircular leading edges at zero incidence in a low turbulence open jet for plate chord/thickness ratios up to 52. The influence of end plates on the Strouhal number has also been studied and it should be noted that the present results have not been subjected to any form of correction for blockage effects.

Without sound, apart from a small change in the chord to thickness ratio at which the abrupt jump in Strouhal number occurs, the data for plates with square leading edges (ie prisms with rectangular cross-sections) agree well with those measured by Nakaguchi *et al*<sup>12</sup> when end plates are fitted. For a prism of square cross-section ( $c/t = 1$ ) there is good agreement with the value given by Vickery<sup>9</sup> while the results for the shortest plate, with end plates fitted, agree well with previously published data for very thin plates normal to the flow<sup>35,36</sup>. The reduction in Strouhal number when the end plates are removed from plates with square leading edges and  $c/t \leq 1.5$  (Fig 2) highlights the sensitivity of the vortex shedding process to flows along the span of the plate.

For plates with square leading edges in the range  $7.6 < c/t \leq 16$ , where the shear layers are permanently reattached, flow visualization without sound applied shows that the 'patches' of fluid containing concentrated vorticity shed from the separation bubbles are randomly distributed in the boundary layers (Fig 7(c)). As reattachment is close to the trailing edge there is little diffusion of the vorticity, and the random arrival of these patches at the trailing edge is probably why no clear regular vortex streets were observed in the region from the trailing edge up to 20 plate thicknesses downstream.

The very long plates with either square or semicircular leading edges ( $c/t$  of 25 and 52) shed vortices at practically the same frequencies and the values for the latter group form a smooth curve with the results for shorter plates (Fig 2). This indicates that a distance of about 25 plate thicknesses is required before the boundary layer characteristics which affect vortex shedding are insensitive to the differences in the leading edge geometry. These lengths agree with the observations of the time averaged boundary layer characteristics on a long flat plate with a square leading edge reported by Ota and Itasaka<sup>10</sup> and Ota and Narita<sup>41</sup>. Their data showed the reattachment length to be about 5 plate thicknesses while development to a fully developed, flat plate turbulent boundary layer condition required about 14 plate thicknesses for the mean velocity profile and more than 18 plate thicknesses for the turbulence velocities and turbulent shear stress profiles.

### Separation bubble size and natural vortex street formation

That two square leading edged plates of the same  $c/t$  ratio (3.16) shed vortices in different regimes

according to the plate thickness, and that the thicker plate can be made to shed intermittently in both regimes by the addition of end plates highlight the sensitivity of the transition between vortex shedding regimes to flow in the spanwise direction. Without end plates installed on the thicker plate, more fluid penetrates the separation bubble in a spanwise direction. This increases the length to reattachment and thus prevents the intermittent shear layer reattachment which is a necessary condition for the plate to shed vortices naturally in regime 'b'. The difference in  $c/t$  where transition between regimes 'a' and 'b' occurs in the present tests and that observed by Nakaguchi *et al*<sup>12</sup> is almost certainly due to differences in the three-dimensional aspects of the test arrangements and their influence on the spanwise flows.

### Smoke and smoke probe effects on vortex shedding frequency

Flow structures in the plate boundary layers downstream of the leading edge are much larger than those induced by the mixing of the gases upstream of the plate to produce the smoke<sup>42</sup>. The insensitivity of the vortex shedding frequency to the presence of these smaller structures, when the smoke is introduced either from above or below the plate, suggests they have a negligible influence on the vortex shedding process. The increase in the vortex shedding frequency when the smoke probe intersected the upstream stagnation streamline is consistent with the results of Laneville, Gartshore and Parkinson<sup>43</sup>.

### Effect of sound on vortex shedding

In drawing conclusions from the observations reported in this paper when sound was applied, two limitations on the range of the applied sound should be noted. First, the maximum sound pressure levels and acoustic velocities were small compared with the pressure and velocity amplitudes frequently recorded in acoustic or mechanical resonance conditions. Second, the frequency range of the applied sound was limited with the highest sound frequencies corresponding to Strouhal numbers less than 0.36.

For the shorter plates in each group (square leading edges with  $c/t < 3.0$ , semicircular leading edges with  $c/t < 1.2$  and the circular cylinder) the sound applied had no significant effect on the vortex shedding process; this is consistent with previous observations by other workers<sup>3,4,26</sup>. For all longer plates ( $c/t$  up to 16) where the shear layers naturally reattach to the plate, the principal influence of applied sound is to move the reattachment position closer to the leading edge. The magnitude of this change increases with both frequency and sound pressure level. For plates with square leading edges, the natural oscillations in the length of the leading edge separation bubbles are suppressed by the application of sound and are replaced with oscillations at the sound frequency. Each bubble grows and divides once per acoustic cycle forming patches of high vorticity fluid which move towards the trailing edge

in the boundary layers of the plate. These discrete vorticity patches arrive at the trailing edge, alternately from each side of the plate, and interact to form a vortex street which is shed at the sound frequency with a relatively small formation region.

An intermediate case arises with square leading edge plates in regime 'b' ( $3.2 \leq c/t \leq 7.6$ ) when the natural vortex formation process without applied sound involves intermittent reattachment of the shear layers during each vortex formation cycle. If sound is applied at a relatively low frequency (similar to the frequency of natural vortex formation) it has little influence on the vortex formation process. This applies up to the frequency at which the shortening of the separation bubble is sufficient to cause reattachment to the plate surface throughout the whole cycle. Here, the vortex shedding is changed to that experienced on longer plates and the application of sound at higher frequencies produces a corresponding stable vortex street with a Strouhal number equal to the applied sound Strouhal number (Fig 9). For slightly longer plates with square leading edges ( $7.6 < c/t \leq 16$ ) in the presence of sound, the separation bubbles fluctuated in length in a regular manner at the sound frequency. The fluctuations in bubble length were  $180^\circ$  out of phase on opposite sides of the plate and the vorticity patches generated by the bubbles growing and dividing were distributed in a regular pattern in the boundary layers. These concentrations of vorticity were synchronized to arrive at the trailing edge alternately from each side of the plate, which permits a vortex street to be shed at the sound frequency when the sound is applied over a wide frequency range.

For cases in which the applied sound causes vortices to form at the sound frequency, the effect extends to the highest frequencies applied but, above a certain limiting value (Strouhal number depending on  $c/t$  but always close to 0.21), the resultant vortex street is not stable near the plate's trailing edge. The vortices break down and a new vortex street then forms further downstream with increased vortex spacing (and a lower corresponding Strouhal number). This is similar to the observations made by Bearman and Davies<sup>44</sup> when oscillating a triangular cylinder with the vertex pointing downstream.

The effect of an acoustic field on the position of shear layer reattachment cannot be explained by a quasi-steady flow model<sup>45</sup>.

## Acknowledgements

The authors wish to thank Mr. N. B. Hamilton for photographing the flows presented in this paper, and Professor A. R. Oliver and Dr. G. R. Walker for their helpful discussions during this investigation. Dr. Parker also wishes to thank CSIRO for the use of its facilities and for making it possible for him to work in their laboratory in Melbourne, Australia.

## References

1. Strouhal V. Über eine besondere Art der Tonerregung. *Ann. Phys. und Chemie, New Series*, 1878, 5, 216
2. Gerrard J. H. Measurements of sound from circular cylinders in an airstream. *Proc. Phys. Soc. B.*, 1955, 68, 453
3. Gerrard J. H. An experimental investigation of the oscillating lift and drag of a circular cylinder shedding turbulent vortices. *J. Fluid Mech.*, 1961, 11, 244
4. Gerrard J. H. A disturbance-sensitive Reynolds number range of the flow past a circular cylinder. *J. Fluid Mech.*, 1965, 22, 187
5. Gerrard J. H. The mechanics of the formation region of vortices behind bluff bodies. *J. Fluid Mech.*, 1966, 25, 401
6. Gerrard J. H. Numerical computation of the magnitude and frequency of the lift on a circular cylinder. *Phil. Trans. Roy. Soc.*, 1967, A1118, 261
7. Bearman, P. W. On vortex street wakes. *J. Fluid Mech.*, 1967, 27, 625
8. Bearman P. W. On vortex shedding from a circular cylinder in the critical Reynolds number regime. *J. Fluid Mech.*, 1969, 37, 577
9. Vickery B. J. Fluctuating lift and drag on a long cylinder of square cross-section in a smooth and in a turbulent stream. *J. Fluid Mech.*, 1966, 25, 481
10. Ota T. and Itasaka M. A separated flow on a blunt flat plate. *J. Fluids Engng*, 1976, 98, 79
11. Bearman P. W. Review: Bluff body flows applicable to vehicle aerodynamics. *J. Fluids Engng.*, 1980, 102, 265
12. Nakaguchi H., Hashimoto K. and Muto S. An experimental study on aerodynamic drag of rectangular cylinders. *J. Japan Aeronaut. Space Sciences*, 1968, 16, 1
13. Bearman P. W. and Trueman D. M. An investigation of the flow around rectangular cylinders. *Aeronaut. Q.*, 1972, XXII, 229
14. Sarpkaya T. Vortex-induced oscillations. *J. Appl. Mech. ASME*, 1979, 46, 241
15. Sarpkaya T. and Shoaff R. L. An inviscid model of two dimensional vortex shedding for transient and asymptotically steady separated flow over a cylinder. *AAIA, 17th Aerospace Sciences Meeting. New Orleans*, 1979
16. Clements R. R. An inviscid model of two-dimensional vortex shedding. *J. Fluid Mech.*, 1973, 57, 321
17. Griffin O. M. and Ramberg S. E. The vortex-street wakes of vibrating cylinders. *J. Fluid Mech.*, 1974, 66, 553
18. Stansby P. K. The locking-on of vortex shedding to the cross-stream vibration of circular cylinders in uniform and shear flows. *J. Fluid Mech.*, 1976, 74, 641
19. Parker R. Resonant effects in wake shedding from parallel plates: Some experimental observations. *J. Sound Vib.*, 1966, 4, 62
20. Parker R. Low frequency resonance effects in wake shedding from parallel plates. *J. Sound Vib.*, 1968, 7, 371
21. Parker R. Discrete frequency noise generation due to fluid flow over blades, supporting spokes and similar bodies. *ASME, Paper No. 69-WA/GF13*, 1969
22. Parker R. and Llewelyn D. Flow induced vibration of cantilever mounted flat plates in an enclosed passage: An experimental investigation. *J. Sound Vib.*, 1972, 25, 451
23. Parker R. and Pryce D. C. Wake excited resonances in an annular cascade: An experimental investigation. *J. Sound Vib.*, 1974, 34, 247
24. Welsh M. C. and Gibson D. C. Interaction of induced sound with flow past a square leading edged plate in a duct. *J. Sound Vib.*, 1979, 67, 501
25. Archibald F. S. Self excitation of an acoustic resonator by vortex shedding. *J. Sound Vib.*, 1975, 38, 81
26. Peterka J. A. and Richardson P. D. Effects of sound on separated flows. *J. Fluid Mech.*, 1969, 37, 265
27. Bloor M. S. The transition to turbulence in the wake of a circular cylinder. *J. Fluid Mech.*, 1964, 19, 290
28. Nagano S., Naito M. and Takata H. A numerical analysis of two-dimensional flow past a rectangular prism by a discrete vortex model. *Euromech 119, 1979. Reported J. Fluid Mech.*, 1980, 99, 225

29. **Graham J. M. R.** The effect of end plates on the two-dimensionality of a vortex wake. *Aeronaut. Q.*, 1969, **XX**, 237
30. **Cowdrey C. F.** A note on the use of end plates to prevent three-dimensional flow at the end of bluff cylinders. *A.R.C.23*, 1962, 907 *F.M.3206*
31. **Parker R.** Resonant effects in wake shedding from parallel plates: calculation of resonant frequencies. *J. Sound Vib.*, 1967, **5**, 330
32. **Bassett R. W. and Fowler H. S.** Improvements to a smoke generator for use in wind tunnels. *N.R.C. Report*, 1971, 12288
33. **Hama R.** Streamlines in a perturbed shear flow. *Phys. Fluids*, 1962, **5**, 644
34. **Michalke A.** On spatially growing disturbances in an inviscid shear layer. *J. Fluid Mech.*, 1965, **23**, 521-544
35. **Fage A. and Johansen F. C.** On the flow of air behind an inclined flat plate of infinite span. *Proc. Roy. Soc.*, 1927, *Series A*, 116
36. **Roshko A.** On the drag and shedding frequency of two-dimensional bluff bodies. *NACA*, 1954, *Technical Note* 3169
37. **Howe M. S.** Contributions to the theory of aerodynamic sound, with application to excess jet noise and the theory of the flute. *J. Fluid Mech.*, 1975, **71**, 625
38. **Bradshaw P. and Wong F. Y. F.** The reattachment and relaxation of a turbulent shear layer. *J. Fluid Mech.*, 1972, **52**, 113
39. **Blevins R. D.** Flow-induced vibration. *Van Nostrand Reinhold Company*, 1977
40. **Welsh M. C., Parker R. and Stoneman S. A. T.** Interaction between vortex shedding and acoustic resonance. *Euromech 119*, 1979. *Reported J. Fluid Mech.*, 1980, **99**, 225
41. **Ota T. and Narita M.** Turbulence measurements in a separated and reattached flow over a blunt flat plate. *J. Fluid Engng.*, 1978, **100**, 224
42. **Perry A. E. and Lim T. T.** Coherent structures in coflowing jets and wakes. *J. Fluid Mech.*, 1978, **88**, 451
43. **Laneville A., Gartshore I. S. and Parkinson G. V.** An explanation of some effects of turbulence on bluff bodies. *Proc. 4th Int. Conf. on Wind Effects on Buildings and Structures*, 1975, *Cambridge University Press*, (1977), 333
44. **Bearman P. W. and Davies M. E.** The flow about oscillating bluff structures. *Proc. 4th Int. Conf. on Wind Effects on Buildings and Structures*, 1975, *Cambridge University Press*, (1977), 285
45. **Sam R. G., Lessmann R. C. and Test F. L.** An experimental study of flow over a rectangular body. *J. Fluid Engng.*, 1979, **101**, 443



## CALENDAR

**Heat Exchangers for Two-phase Applications (Part of ASME-AIChE National Heat Transfer Conference)** 24-28 July 1983  
Seattle, WA, USA

**21st National Heat Transfer Conference** 24-28 July 1983  
Seattle, WA, USA

**3rd International Conference on Numerical Methods in Thermal Problems** 2-5 August 1983  
Seattle, WA, USA

**Numerical Methods in Laminar and Turbulent Flow** 8-11 August 1983  
Seattle, WA, USA

**18th Intersociety Energy Conversion Engineering** 21-26 August 1983  
Orlando, FL, USA

**Measurement Techniques in Power Engineering** 29 Aug-5 Sept 1983  
Dubrovnik, Yugoslavia

**ELSI VI (6th International Conference on Erosion by Liquid and Solid Impact)** 4-8 September 1983  
Cambridge, UK

**XVI Biennial Fluid Dynamics Symposium** 4-10 September 1983  
Warsaw, Poland

**Heat and Mass Transfer Techniques (XV ICHMT Symposium)** 5-9 September 1983  
Dubrovnik, Yugoslavia

**2nd International Conference on Cavitation** 6-8 September 1983  
Edinburgh, UK

**3rd International Symposium on Flow Visualisation** 6-9 September 1983  
Ann Arbor, MI, USA

**4th Symposium on Turbulent Shear Flows** 12-14 September 1983  
Karlsruhe, FRG

J. M. Robertson, HTFS, B.392, AERE, Harwell, Oxfordshire, UK, OX11 0RA

J. Chiffreller, AIChE Meetings Department, 345 East 47th Street, New York, NY 10017, USA

Dr R. W. Lewis, Department of Civil Engineering, University College of Swansea, Singleton Park, Swansea, UK, SA2 8PP

Dr C. Taylor, Department of Civil Engineering, University College of Swansea, Singleton Park, Swansea, UK, SA2 8PP

W. R. Martini, Martini Engineering, 2303 Harris, Richland, Washington, USA

International Centre for Heat and Mass Transfer, PO Box 522, 11001 Belgrade, Yugoslavia

J. E. Field, ELSI Conference, Cavendish Laboratory, Hadingly Road, Cambridge, UK, CB3 0HE

Polish Academy of Sciences, Institute of Fundamental Technological Research, Swietokrzyska 21, 00-049 Warsaw, Poland

International Centre for Heat and Mass Transfer, PO Box 522, 11001 Belgrade, Yugoslavia

Conference Department, The Institution of Mechanical Engineers, 1 Birdcage Walk, Westminster, London SW1H 9JJ, UK

Professor Wen-Jei Yang, Department of Mechanical Engineering and Applied Mechanics, The University of Michigan, Ann Arbor, MI 48109, USA

B. E. Launder, Department of Mechanical Engineering, UMIST, Manchester, UK, M60 1QD